5. Industrial slag sample investigations

5.1. Introduction

As indicated previously, metal droplet entrainment has been identified as a possible important factor influencing vanadium recovery to the slag. So far, only the effect of slag basicity on the soluble vanadium loss has been discussed. An alteration of the slag composition by adding less CaO will lower the soluble vanadium loss, but inevitably also changing the separation of the solid ferrovanadium phase from the slag phase. One way to assess the effect of slag basicity on metal droplet entrainment is to investigate solidified industrial slag samples.

In addition, the effect of slag basicity on soluble vanadium loss can be compared to the equilibrium results obtained. The purpose of this investigation is, thus, to identify all the phases co-existing in the industrial slag samples as well as to quantify the amounts of vanadium associated with the oxidic and metal phases respectively.

5.2. Oxidic phase analysis

5.2.1. Experimental procedure

5.2.1.1. Sample preparation

A number of factors such as cooling rate, tap temperature and slag volume influence the amount of entrained metal droplets. The amount of entrained droplets is also influenced by the location of the slag samples taken from the bulk slag (i.e. slag closer to the refractory lining solidifies more quickly, resulting in a larger amount of entrained particles). Nevertheless, by taking slag samples at a fixed location within the slag, the effect of slag basicity on droplet entrainment can be assessed semi-quantitatively.

The vertical segregation effect was addressed by investigating the best and worst positions regarding vanadium loss as entrained droplets, by sampling from the top and bottom, at a fixed horizontal position, in the bulk slag sample. See figure 50 below.

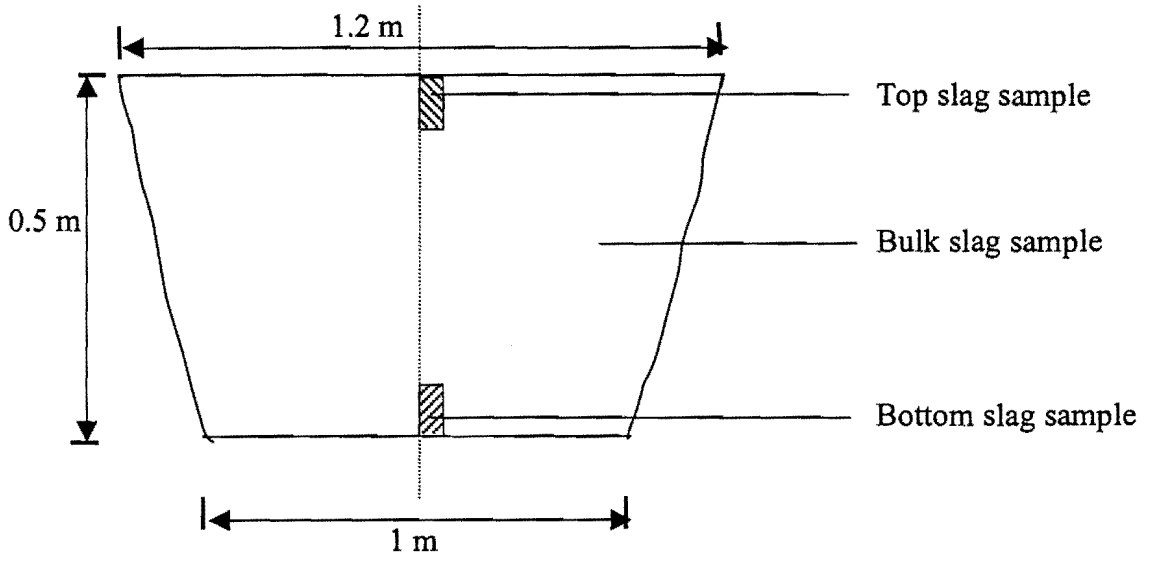

Figure 50: Schematic diagram of a vertical section through the bulk sample showing the location of the samples taken.

To investigate the possible influence of tap temperature on vanadium loss, the slag temperature was also recorded prior to tapping. The temperature readings were taken of the slag pool near the electrodes, through an observation window in the shell, seconds after the arc had been extinquised, using an infra-red pyrometer. Temperature readings of the tap stream could not be obtained due to large dust emissions surrounding the metal tap stream.

The sections were epoxy-impregnated under vacuum, polished, carbon coated and analyzed. Analyses of the oxidic and metal phases were by X-ray diffraction spectroscopy (XRD) and energy dispersive X-ray Spectrometry (EDX). Parts of the samples were milled into powder for XRD analysis. Electron probe microanalyses were done on polished sections using a Jeol 5800 Scanning Electron microscope. Back-scattered electron imaging was first employed to identify all the possible phases, including metal droplets, before quantitative EDX analysis was performed. At first, at least 30 fields were analyzed for a given phase to establish a good mean and small standard deviation. Due to the homogenous nature of the oxidic phases, 10 analyses proved to be sufficient to

establish a good aggregate, and small standard deviation. The following section will focus on investigations performed on the oxidic phase constituent of the slag.

The average chemical composition of the slag samples was determined by performing EDX analysis at the lowest obtainable magnification of 85x. Metal droplets were included in the analysis contributing to higher apparent vanadium levels in the slag. The way in which this was taken into account is discussed later. It was not possible to exclude the metal particles, without raising the magnification and losing the representative nature of the analysis. Around 10 fields were analyzed to establish a good mean and small standard deviation.

5.2.2. Results and discussion

5.2.2.1. Oxidic phase investigations

A back scattered electron image of a slag sample is shown in figure 51:

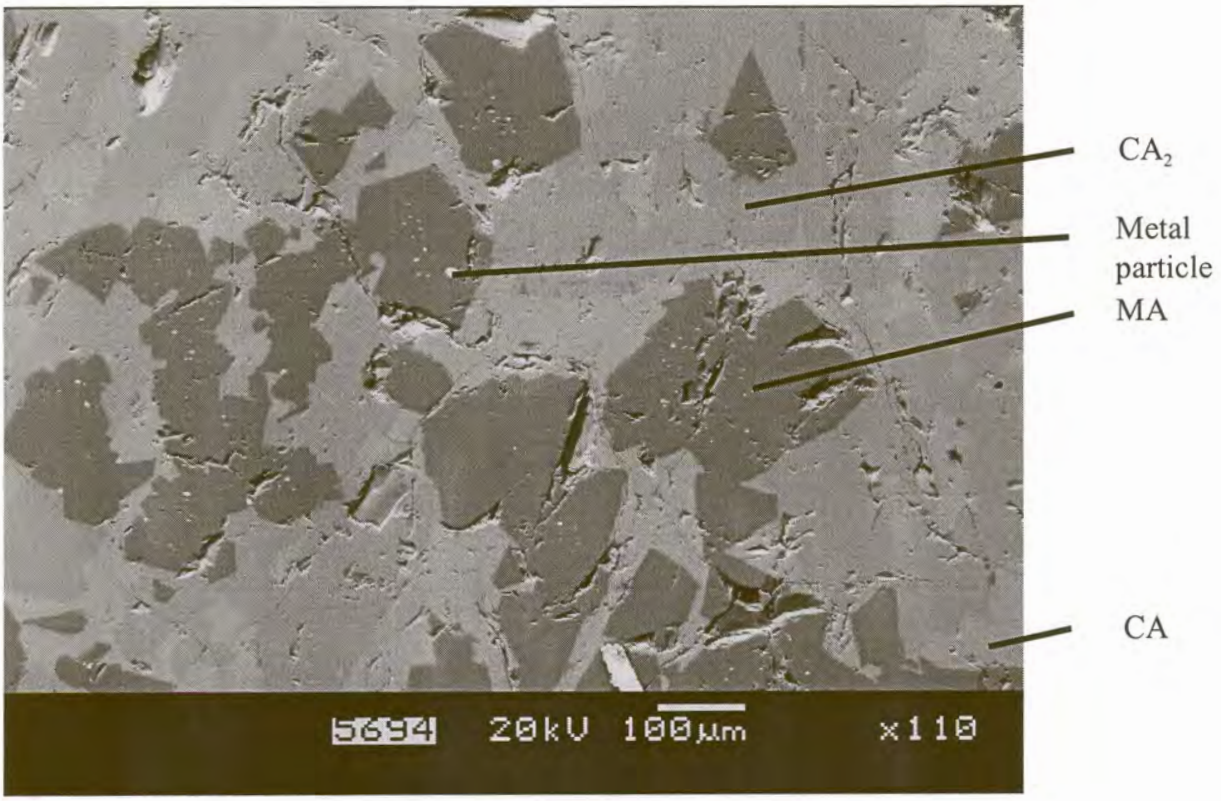

Figure 51: Back-scattered electron image showing the three prominent phases.

The three oxide phases which are visible in figure 51 were identified – based on X-ray diffraction and EDX analysis – as $MgO.Al_2O_3$ (MA), $CaO.Al_2O_3$ (CA), and $CaO.2Al_2O_3$ (CA_2)

All three the phases identified were present in all the slag samples investigated. A fourth phase, shown in figure 52, which is a result of impurities (especially Na) introduced by the vanadium starter material, was also identified in some of the slag samples. Na_2CO_3 or Na_2SO_4 is used as a roasting reagent to react with V_2O_5 in the magnetite ores to form soluble sodium vanadates. Both V_2O_5 and V_2O_3 used as starter vanadium oxide materials in ferrovanadium production are products of the roast / leach process utilized to recover vanadium from ore and vanadium-rich slags. Vanadium pentoxide is mainly exported while V_2O_3 and small quantities of V_2O_5 are used to produce ferrovanadium.

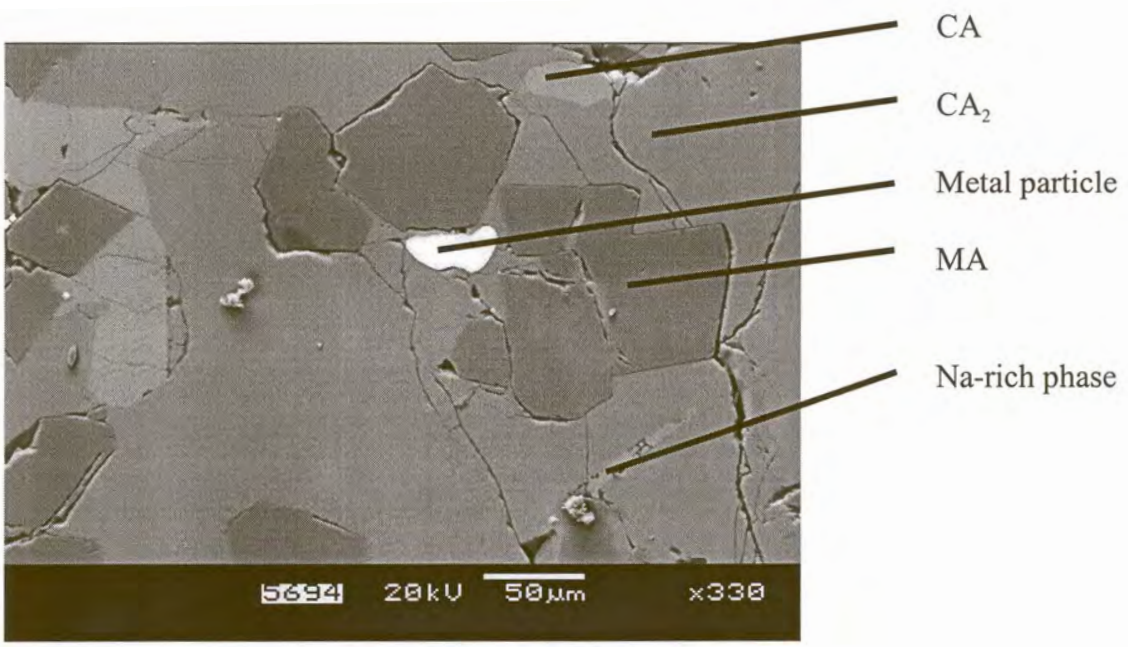

Figure 52: Back-scattered electron image showing the Na – rich phase.

This Na-rich phase usually constituted less than 1 volume % of the slag sample. From time to time vanadium oxide of poor quality was used to produce ferrovanadium, leading to the slag structure shown in figure 53.

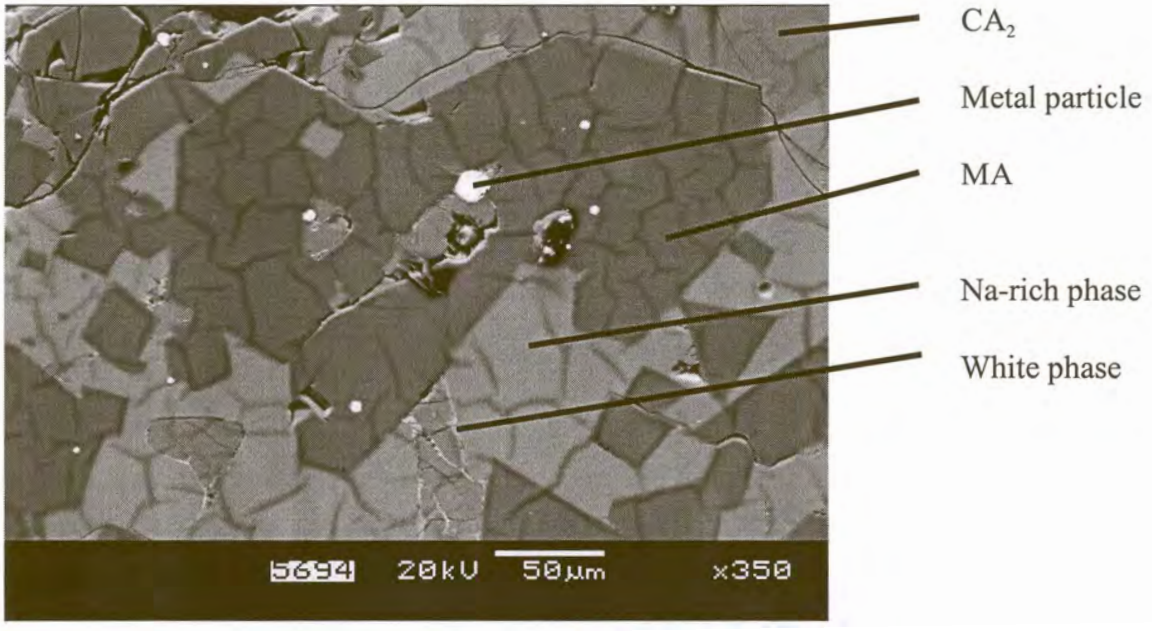

Figure 53: Back – scattered electron image showing a severe case of poor quality vanadium oxide starter material used to produce ferrovanadium.

This figure clearly indicates the Na-rich phase to be present in much larger quantities compared to figure 52. Fortunately, no oxidic vanadium is associated with this phase as indicated by the results shown in Appendix 3 (See slag 7). The detrimental effect of Na in raw material is thus related to higher energy requirements, due to the decrease in exothermicity of the charge, and possibly refractory wear.

For the slags without Na_2O contamination, the locus of the average slag composition lies within the CA-CA_2-MA alkemade triangle, in the primary phase field of MA. During the first stage of crystallization only MA will crystallize from the melt and only solid and liquid will be present, thus enabling crystals of MA to grow. The primary crystals of MA will be large and have an idiomorphic shape since the melt does not hinder their crystallization. The idiomorphic shape of the MA crystals can clearly be seen in figure 51.

It can be concluded that solidification of the ferrovanadium slag follows (to an extent) equilibrium cooling (if the Na-rich phase is neglected, based on the small quantities usually occurring in the slag).

Interestingly, the metal particles occur only on the boundary or within the MA phase as indicated by both figures 51 and 52. The metal droplets (containing mainly V, Fe and Al) have a higher liquidus temperature than the slag (see figure 17), resulting in metal solid formation while the slag is still in the liquid state. On subsequent solidification, the solid metal particles may serve as seed crystals for nucleation of the MA phase, resulting in their occurrence within or on the boundary of the MA phase. It can be concluded that metal droplets occurring in any other phase except the MA phase, are probably the result of entrainment after primary crystallization. This may occur during any slow tapping when molten ferrovanadium is tapped onto semi-solidified slag. The $MgO.Al_2O_3$ (MA) phase was found to be the major repository of oxidic vanadium containing up to 6% V_2O_3 (on a molar basis), compared with less than 0.4% in the CA and CA_2 phases. (See Appendix 3 for chemical analyses)

The calculated chemical composition based on EDX analysis indicates the Al_2O_3-content of the MA phase to vary between 70 and 75%, compared to the (stoichiometric) 72% obtained from the ternary phase diagram. The MgO content of the MA phase never

exceeds 24% (on a mass basis) compared to the 28% given by the phase diagram. The MgO-content of the MA phase is therefore distinctly lower than in the equilibrium MA phase. The MA phase was confirmed, by XRD analysis, to have a spinel-type structure. The general formula of the spinel can be written as $A^{2+}B_2^{3+}O_4$, where A^{2+} can be iron, chromium, magnesium, zinc, vanadium and manganese, and B^{3+} can be aluminium, iron, chromium or vanadium. Vanadium can therefore substitute either magnesium or aluminium in the spinel-type lattice to form a solid solution without altering the lattice spacing of the structure much. The dominant oxidation states of vanadium can be either V^{2+} or V^{3+}.

Such substitution can be clarified by plotting the normalized Mg and V cation fractions of the MA phase - as obtained by EDX analysis- against the Al fraction, as shown in figure 54.

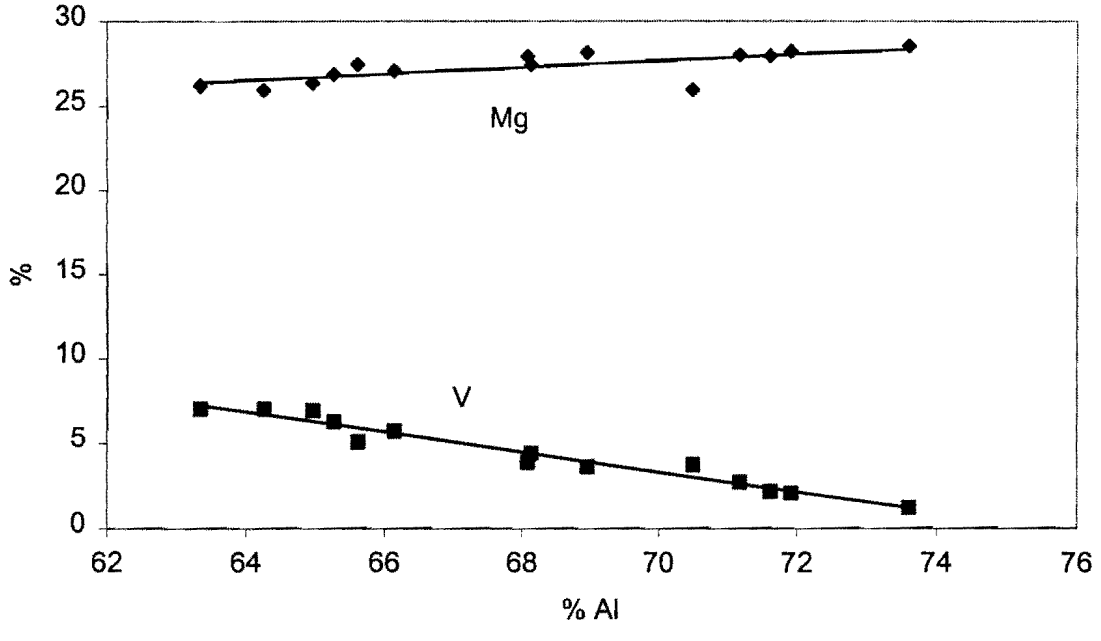

Figure 54: The effect of the Al cation fraction on the fractions of Mg and vanadium in the MA phase as obtained by EDX analysis (mole percentages).

Figure 54 clearly indicates that vanadium substitutes mainly aluminium in the spinel-type structure. The partial substitution vanadium of magnesium is also evident because the actual Mg^{2+} fraction is lower than the expected 31 %. The dominant oxidation state of vanadium in the structure would therefore be V^{3+}. The Al_2O_3 content of the MA phase has

therefore a strong effect on the vanadium content of this phase, as indicated by figure 55 which shows the calculated oxide fractions of the equilibrium MA phase.

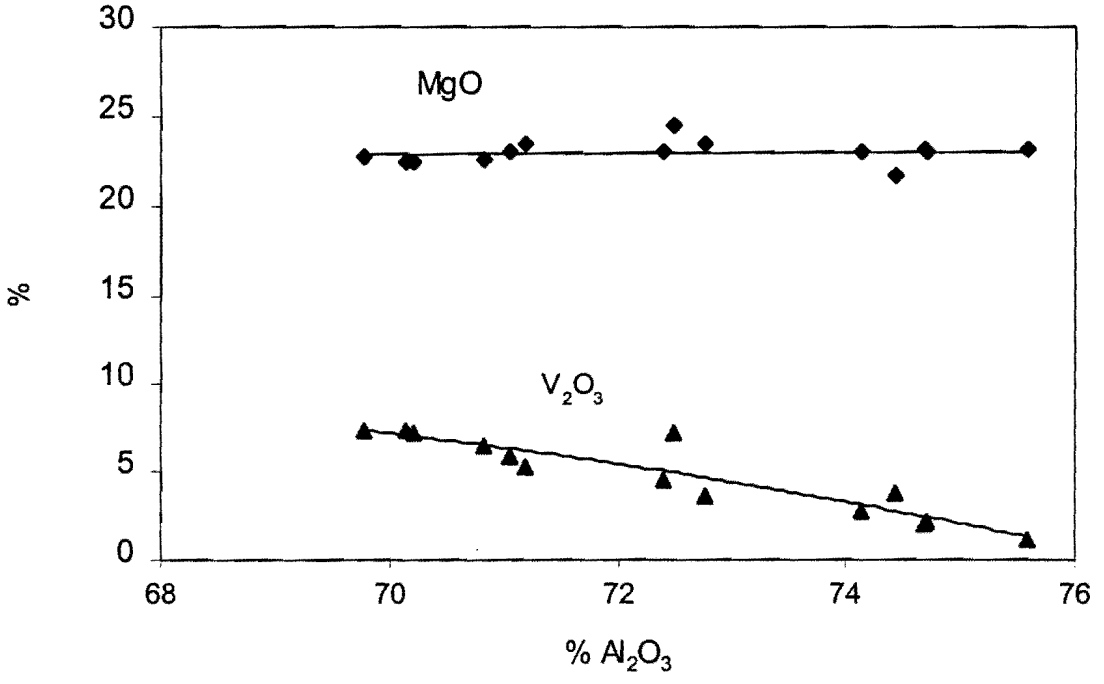

Figure 55: Recalculated chemical compositions of the MA phases showing the effect of alumina on the V_2O_3 content of these phases (mass percentage).

In conclusion, vanadium is associated in the solid state with primarily the MA spinel-type phase where V_2O_3 substitutes Al_2O_3 in this structure to form a solid solution without altering the lattice spacing of the structure much (as deduced from the XRD results). High alumina contents of the ferrovanadium slags are beneficial for the solid state as well as the liquid state interactions between the vanadium and the slags. Furthermore, the MgO content of the slag should be reduced, if possible, to inhibit the formation of the MA phase. However the amount of oxidic vanadium will not necessarily be reduced if the amount of MA phase is reduced because the MA phase can contain up to 6% V_2O_3. In other words, a small amount of MA phase with a high vanadium content can result in a high overall vanadium content in the slag. Nevertheless, vanadium losses are predicted to be much lower for slags with lower CaO and MgO contents due to the similarly strong basic nature of these oxides (as discussed in a previous chapter). Although the effect of the MgO content on the vanadium activity coefficient is not known, the section on equilibrium simulation calculations will incorporate the effect of MgO on the alumina activity which influences the oxidic vanadium content of the slag.

5.2.2.2. Composition relations of the oxidic phase

High temperature equilibrium experiments performed indicate a very strong relationship between the slag composition and the amount of oxidic vanadium in the slag, especially where CaO: $Al_2O_3 < 0.7$ (molar basis). The aim of this section is to determine whether the strong effect of slag basicity on the amount of oxidic vanadium also holds for the industrial slag samples. Because of the higher analyzed vanadium content of the slag sample due droplets included during EDX analysis, the contribution of the metal droplets needed to be quantified. This was done by performing mass balances using the average chemical compositions of each phase, including the droplets, as well as the mean chemical composition of each slag sample. All the vanadium which could not be attributed to the oxidic phases was assigned to the metal droplet phase.

It is worth mentioning at this stage that the analysed vanadium assigned to the metal phase is not the exact amount of vanadium associated with the droplets but just a mere fraction of that amount due to different volumes analyzed by EDX, as shown in figure 56.

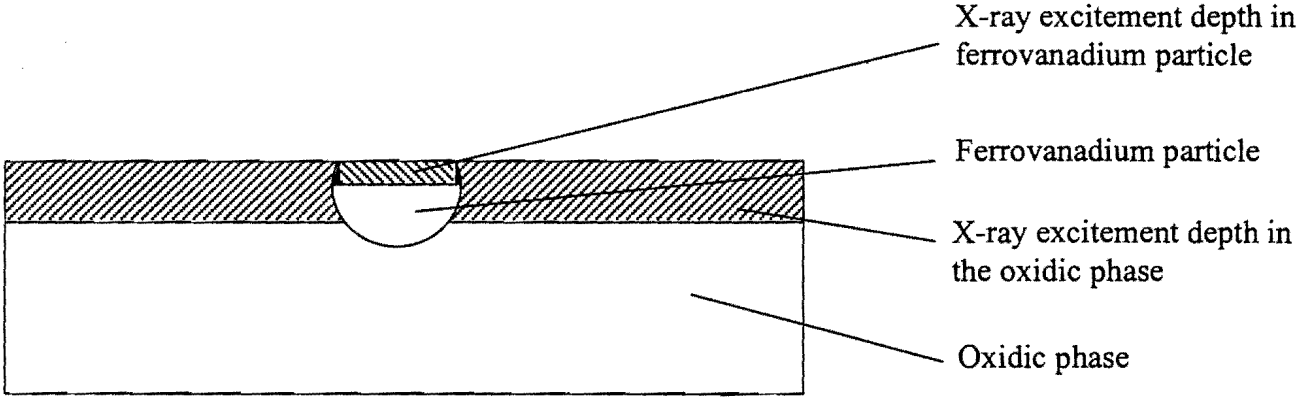

Figure 56: Cross section through a slag sample showing the excitement depth of the oxidic and metal phases in schematic form.

The schematic shows that the excitement depths of metal particles are not as deep compared to oxidic phases An indication of the depth dimension of the interaction volume is given by the following expression (Goldstein et al.,1981)

$$R = 0.0276\ AE_o^{1.67} / Z^{0.889}\rho \quad \mu m \qquad (43)$$

where E_o is given by keV, A in g/mol, ρ in g/cm^3, and Z is the atomic number of the target. Both ρ and Z are higher for metal droplets resulting in a lower depth of excitement, as shown in figure 56. A smaller volume of the metal droplets is exited resulting in lower analysed vanadium levels that would have been obtained if the same depth of excitement had occurred. Thus, only a fraction of the total amount of vanadium present in the metal phase is analysed for if a low magnification EDX analysis is performed. This had no effect on the oxide phase calculations because the Al, Ca and Mg mass balances were performed to estimate the relative amount of each oxide phase and the vanadium balance to determine the amount of vanadium associated with the metallic phase. The results obtained (See Appendices 3 and 4) are summarized in figure 57.

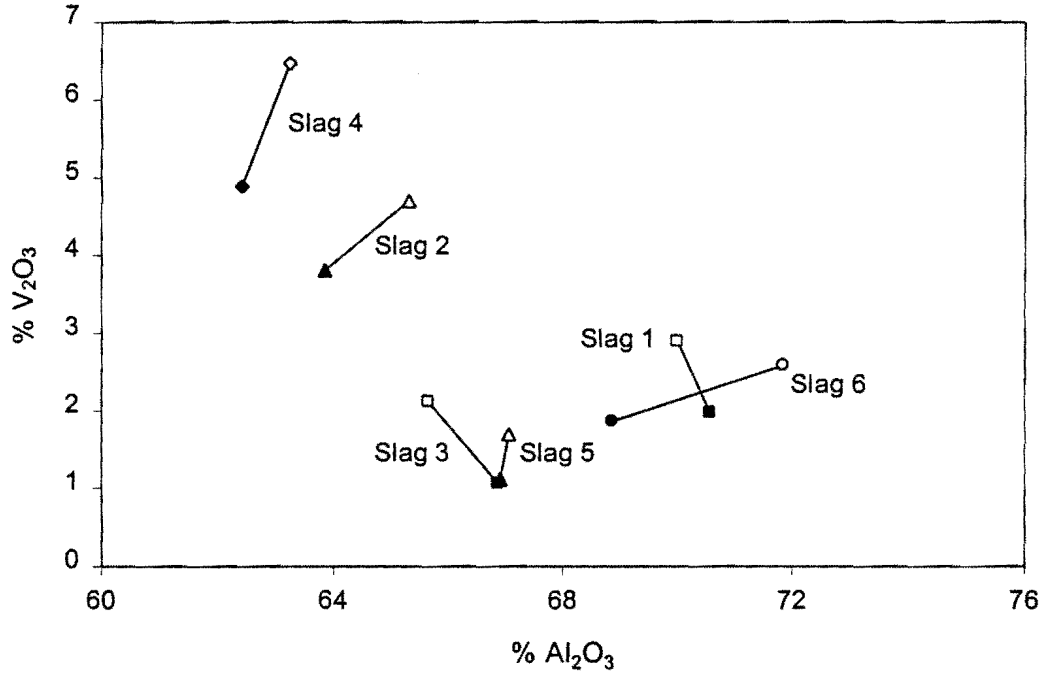

Figure 57: The effect of the alumina content of the industrial slag sample on the oxidic vanadium content. Solid data markers present data of samples taken at the top of the bulk sample and open data markers samples taken from the bottom (mass percentages).

Electric arc smelting processes are known for the poor stirring of the furnace contents resulting in segregation. The segregation of vanadium has an important effect on representative sampling as will be discussed in the next section. The samples taken at the bottom of the bulk slag sample contain up to 1.5% (mass basis) less V_2O_3 compared to the samples taken at the top.

It is not clearly understood whether the segregation indicated by figure 57 is an extension of the segregation in the furnace or a result of the solidification process. Nevertheless, vanadium concentration gradients do occur throughout the bulk slag sample and sampling of the entire bulk sample would be necessary to fully quantify the effect of position on the oxidic vanadium content of the slag. The results obtained in figure 57 (see Appendices 3 and 4) do confirm the laboratory results showing that oxidic vanadium losses are much higher for slags with lower alumina contents. The V_2O_3 content of the slag can be reduced from about 6% to 2% by raising the alumina content from 62% to 67% (mass basis). This confirms the importance of basicity control by control of the CaO additions and MgO refractory wear in such an operation.

5.2.2.3. Industrial slag sampling

The South African ferrovanadium producer under investigation calculates the percentage vanadium recovered per smelt as follows.

$$\% \text{ vanadium recovered} = \frac{\frac{\% V_{FeV}}{100} \times \text{weighed FeV button}}{\frac{\% V_{Hivox}}{100} \times \text{mass of hivox used}} \qquad (44)$$

FeV buttons are the as-cast metal constituent of the electric arc furnace, weighed after shot blasting to remove excess slag (See figure 7). The advantage of this method is that vanadium losses to the slag as oxidic vanadium and entrained droplets are indirectly accounted for by determining the total mass of the button. No time consuming method is necessary to distinguish between the vanadium associated with the slag or entrained metal particles. Thus, this method accounts for all the possible vanadium losses to the slag regardless the type of factor, including reverts (ferrovanadium containing spillages), oxide spillages, metal droplet entrainment or unreduced vanadium oxides, influencing vanadium recovery (See section 2.4.4.). This method is very sensitive regarding the chemical compositions of the hivox and FeV button respectively, and care should be taken that the sampling is representative. Despite the effectiveness of this method, it is absolutely essential for process control purposes that the exact chemical composition of the slag is known. Without the basic knowledge of the chemical compositions of the slag, no process

refinement can be conducted. Strong segregation within the slag sample and the inability of in-line analytical techniques, like the XRF technique, to distinguish between oxidic and metallic vanadium are some of the serious factors hampering the quantitative description of vanadium in the slag.

The ferrovanadium producer under investigation samples the slag prior to tapping by dipping a steel rod into the slag through the observation window in the furnace shell. After dipping, the rod is quickly withdrawn from the slag resulting in the subsequent solidification of the slag onto the rod. Upon cooling the slag is removed from the rod, crushed to a fine powder and sent for X.R.F analysis. Figure 58 shows an electron back-scattered image of such a dipped slag sample.

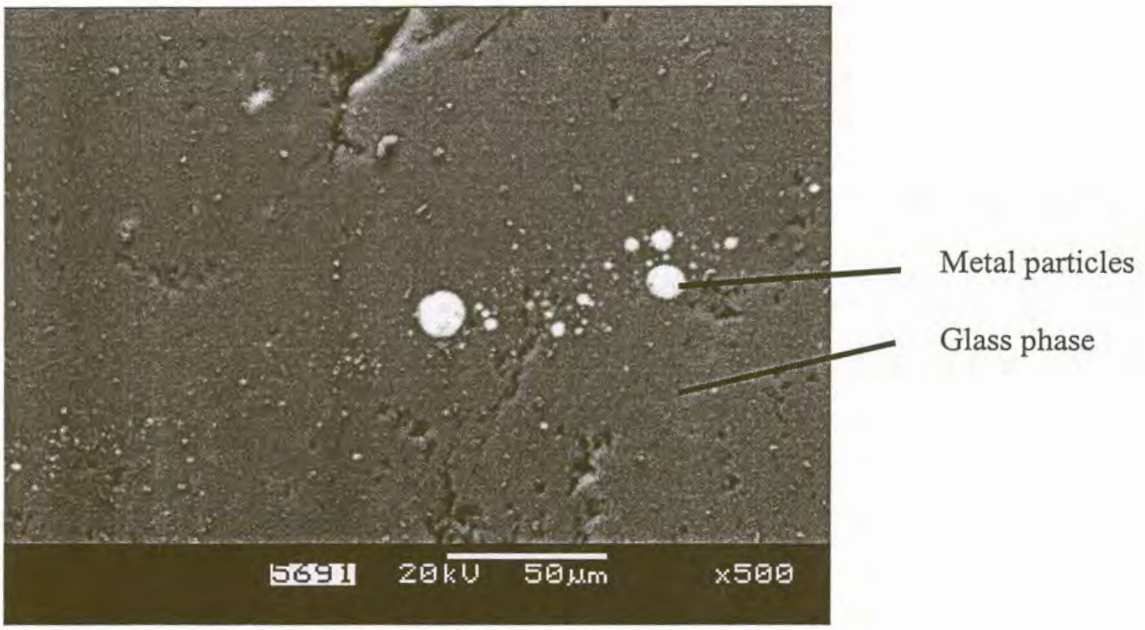

Figure 58: Back-scattered electron image of dipped slag small with metal particles.

This image shows a glass phase formed as a result of very rapid solidification of the thin slag layer on the rod. This image furthermore shows entrained metal particles in the glass phase which must contribute significantly to the average vanadium content of the slag if X.R.F analyses are conducted on the milled dip samples. EDX analysis performed on the entrained metal droplets indicate an average vanadium composition in excess of 93% (See Appendix 5). The absence of Fe in these droplets clearly indicates the poor mixing and

the strong segregation behavior of these slags. This is because initially pure vanadium droplets are formed as a result of the reduction of the vanadium oxide raw materials by aluminium. After agglomeration the pure vanadium droplets form an alloy with the molten scrap iron in the bottom of the furnace. The vanadium detected by X.R.F analysis is therefore likely to be strongly vertical position dependent. The next step is to determine how well the oxidic vanadium content of the dipped sample compares to that of samples taken from the bulk slag sample, at the top and bottom respectively (See slag 6 in Appendices 3 and 4 for chemical analysis), after tapping. A number of pieces of the dipped sample were co-mounted in epoxy resin, polished and analyzed using EDX. Special care had to be taken to ensure that the metal particles were excluded during analysis. At least 40 fields were analyzed to establish a good mean and standard deviation (See Appendix 6 for chemical analysis). The results obtained are summarized in figure 59.

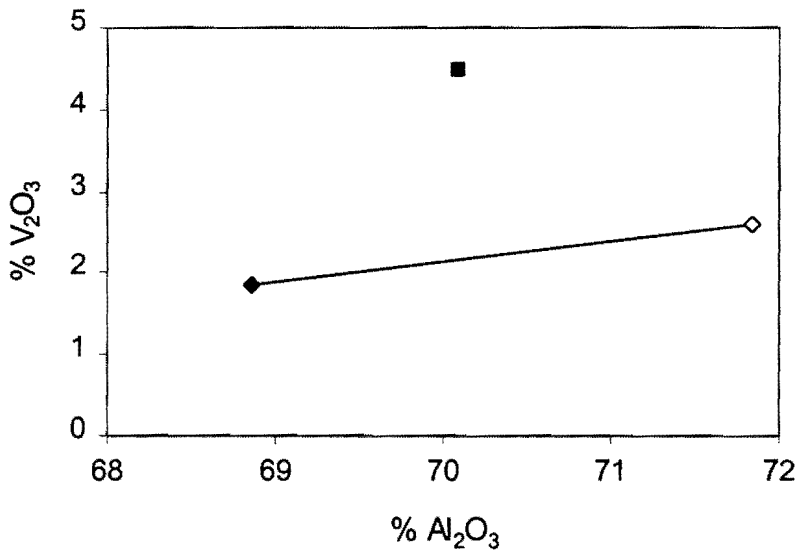

Figure 59: Comparison between vanadium content of dipped sample and samples taken from the bulk solidified sample after tapping. Square data marker represents dipped slag sample and diamond markers samples from the bulk slag sample.

The dipped sample analyzed appreciably higher for V_2O_3 than the two samples taken from the bulk sample. The figure furthermore illustrates that the alumina content of the dipped sample compares well with the average alumina content of the other two samples. The strong segregation behavior of the slag has clear implications for attempts at process refinement because the V_2O_3 content of the slag, determined by X.R.F analysis, may be in

excess of the average vanadium content of the slag. In other words, the in-furnace segregation effect may overshadow any change in vanadium content due to changes made for process improvement. Ways have to be found to address this problem and to ensure that sampling is much more representative of the bulk of the slag. Perhaps one such a way is to sample in the tap stream where the slag is much more subjected to stirring. Further investigations are therefore necessary to address this problem of representative sampling.

5.2.2.4. Industrial X.R.F. relations

Although the vanadium content of the dipped samples is likely to be in excess of the average bulk sample, the industrial X.R.F. analysis may be of some value as long as the sampling procedure is consistent. Historic industrial data, relating to 3 months of production during which in excess of 550 smelts were made, were collected, grouped and are summarized in figures 60-62. The large confidence intervals are a result of extensive scattering of plant data.

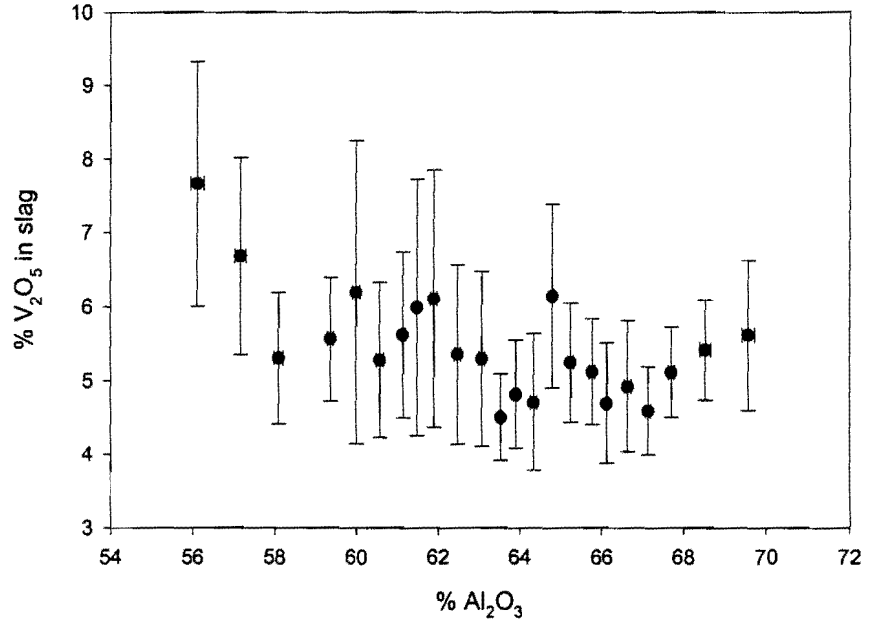

Figure 60 : Total vanadium oxide content as function of the alumina content of the slag based on XRF analyses of dip samples. All the vanadium in slag, including droplets, is reported as V_2O_5.

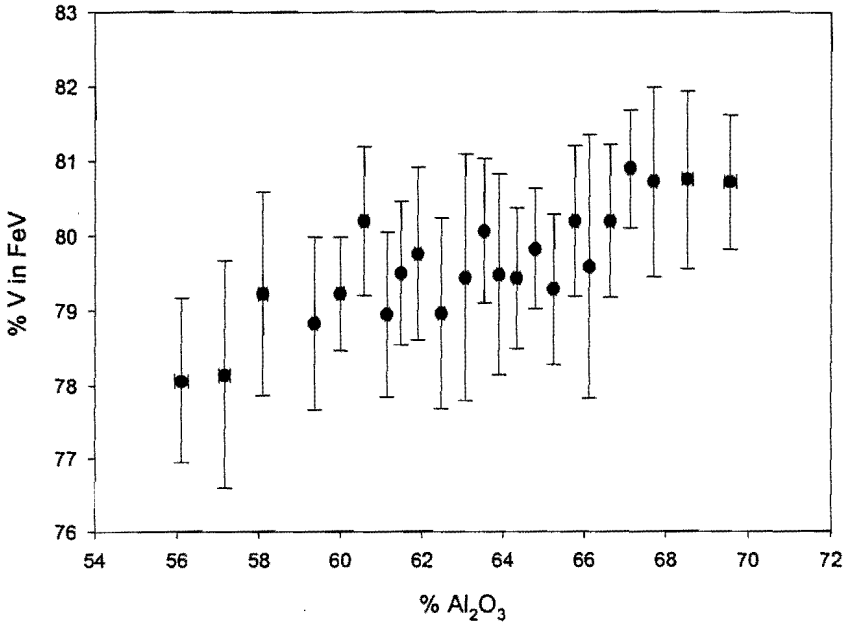

Figure 61: Vanadium content of ferrovanadium as a function of the alumina content of the slag. The XRF analysis technique was used to analise for alumina and vanadium of different dip slag and metal chip samples (taken from the metal buttons), respectively.

Figure 60 shows that high-alumina slags are beneficial for vanadium recovery. The alumina content strongly influences the oxidic amount of vanadium resulting in higher vanadium contents in the metal for increased amounts of alumina in the slag, as depicted by figure 61. In other word high alumina slags result in heavier ferrovanadium buttons with higher vanadium contents. This is in close agreement with the laboratory measurements and EDX results obtained from industrial slag samples.

Because of strict international specifications on the aluminium content of ferrovanadium, some concern may arise on what the effect of higher alumina contents is on the residual aluminium of the ferrovanadium. The effect of higher alumina contents on the vanadium content of the ferrovanadium is shown in figure 62.

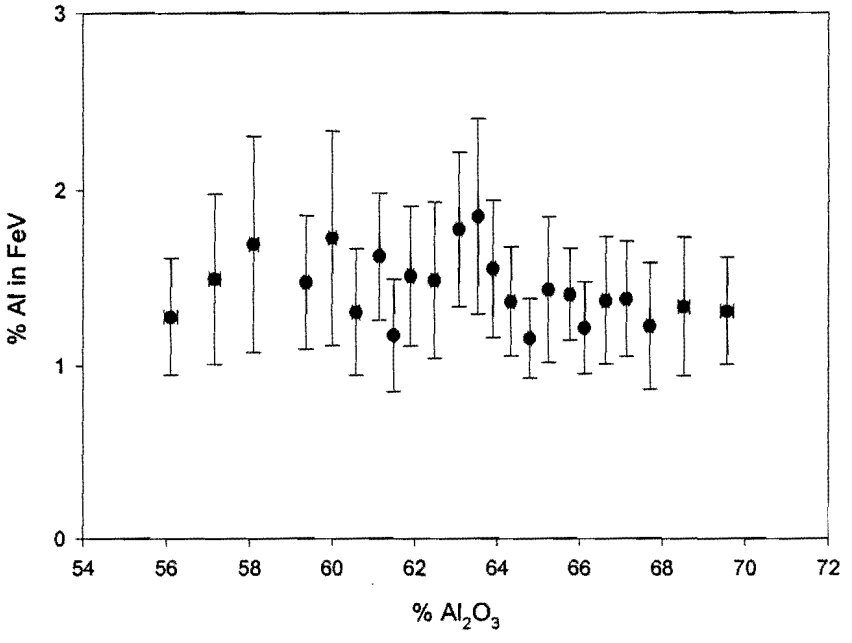

Figure 62: The effect of the slag composition on the aluminium content of the ferrovanadium.

This figure indicates that the aluminium content of the ferrovanadium is expected to remain constant, for slags containing up to 70 % Al_2O_3, if the slag basicity is decreased by lowering the lime additions.

It was previously assumed that MgO (for slags containing from 5 to 15 % of MgO on a mass basis) and CaO are similarly strong basic oxides and would therefore behave similarly in Al_2O_3-rich liquid slags. Because of the scatter in the plant data, no conclusion can be made on this regard. The next section aims to quantify metal droplet entrainment as a possible mechanism of vanadium loss to the slag.

5.3. Metallic phase analysis

5.3.1. Introduction

EDX on industrial slag samples and laboratory results indicate that the Al_2O_3 content of the slag has a strong effect on the soluble vanadium loss to the slag. The decrease of the slag basicity by lowering the lime additions will result in higher liquidus temperatures and hence possibly higher slag viscosities, which may lead to higher metallic losses. It is still uncertain which of the oxidic or metallic loss contributes most strongly to the total vanadium loss in the slag. The aim of this section is to quantify the amount of vanadium typically associated with the metallic phase and to what extent the slag basicity influences metal droplet entrainment.

5.3.2. Experimental procedure

5.3.2.1. Sample preparation

The investigations were carried out on the polished sections (See slags 1-6 in Appendices 3 and 4) previously subjected to oxidic phase analysis, as reported in section 5.2.2.2.

5.3.2.2. Procedure to determine droplet-size distributions and to estimate mass of vanadium associated with the metal particles.

Polished sections were investigated using an optical microscope and photos of the entrained droplets were taken with a digital camera. The y-coordinate of the polished sections (that is vertical in the bulk slag sample) was incrementally increased, while photos were taken randomly along the x-coordinate. Special care was taken to ensure that the photos were representative of the entire sample because of the large difference in the droplet dimensions (0.5 μm - 60 μm apparent diameter). Using the Imagetool software package, the areas of the individual particles as well as the total droplet area expressed as a fraction of the total sample area, were estimated. Subsequently the generated data were used to determine the two-dimensional size distribution of the planar section. Without any additional calculations, the total droplet area fraction can be used to estimate the volume

fraction of metal particles entrained in the slag. The amount of metal droplets in the slag can also be estimated by determining the true spatial size distribution of the droplets entrained in the polished sections. Once the two-dimensional size distribution of the planar section has been determined, equations can be utilized to estimate the spatial size distribution. The true spatial size distribution can be used to determine to what extent each size class interval contributes to the total mass of entrained metal particles. Most of the methods derived to calculate the spatial size distribution make use of the assumption that the particles are spherical. The entrained droplets are almost perfect spheres, as can be seen from the back-scattered images, thus fitting the assumption perfectly. The following correlation was used to calculate the spacial size distribution (Underwood, 1986).

$$N_{v,i} = 1/Di(1.645\ N_{A,i} - 0.4542\ N_{A,i-1} - 0.1173\ N_{A,i-2} - 0.0423\ N_{A,i-3} - 0.01561\ N_{A,i-4} - 0.0083\ N_{A,i-5} - 0.0036\ N_{A,i-6} - 0.0019\ N_{A,i-7} - 0.0009\ N_{A,i-8} - 0.00044\ N_{A,i-9} - 0.00036\ N_{A,i-10} - 0.0001\ N_{A,i-11} - 0.00003\ N_{A,i-12} - 0.00003\ N_{A,i-13} - 0.00001\ N_{A,i-14} \quad (43)$$

$N_{A,i}$ = Planar density of droplets in class interval i (estimated from the planar size distribution) (number/mm^2)

$N_{v,I}$ = Volumetric density of droplets in class interval i (number /mm^3)

Di = maximum droplet diameter in class interval i

Droplet size class intervals were determined by applying the $\sqrt{2}$ - ratio of geometric grouping. This was done by multiplying the pre-determined minimum droplet diameter of the first class interval by $\sqrt{2}$ to establish the upper limit of the size interval. This value was used as the lower limit of the next class interval, for which the upper limit was again calculated by multiplying the lower limit by $\sqrt{2}$. This procedure was repeated until all the droplets could be classed.

The average droplet diameter for each class interval was calculated as the geometric mean of the maximum and minimum diameters of the class interval.

It is further worth mentioning that each class interval should at least contain 7 areas for calculation purposes (Underwood,1986).

5.3.3. Results and discussion

Table 18 gives a summary of the volume % metal particles, droplet composition, droplet and slag densities, mass of vanadium in droplets, percentage oxidic vanadium, mass of V in oxidic phases, total mass of vanadium in slag and the mass percentage V in 1230 kilograms of slag in each slag sample.

Some of the slag samples contained above average-sized entrained metal droplets resulting in the high standard deviations and 95 % confidence limits. Large entrained metal particles hamper representative sample photography because the magnification has to be chosen in such a way that a representative portion of the large particles is included. This causes the small particles not to be optically resolved. This problem was overcome by choosing a magnification which enabled the small particles to be just identified and the number of photographs that was taken, was increased substantially. Nevertheless, some of the large standard deviations could not be substantially reduced.

Slag	Volume % droplets	Standard Deviation	95 % Confidence limits	Droplet composition			Dencities(g/cm^3)		Mass V in droplets (kg)	% V in slag	Mass of oxidic V	Total mass V	% V_T (1230 kg)
				% Al	% V	% Fe	Droplet	Slag					
Slag 1 top	0.10	3.13	1.37	0.1	95	4.90	6.02	3.80	1.80	2.31	28.43	30.23	2.46
Slag 1 bottom	0.87	0.14	0.06	0.2	95	4.80	6.02	3.80	16.02	2.31	28.43	44.44	3.61
Slag 2 top	0.19	0.24	0.11	5.80	83.6	4.40	5.98	3.81	2.99	2.65	32.61	35.60	2.89
Slag 2 bottom	0.22	0.22	0.10	1.12	77.8	16.54	6.42	3.81	3.61	2.38	29.26	32.87	2.67
Slag 3 top	0.15	0.10	0.05	7.34	74.2	8.81	6.14	3.81	2.16	1.56	19.23	21.39	1.74
Slag 3 bottom	1.01	1.33	0.71	2.85	81.5	8.82	6.31	3.79	16.88	0.68	8.36	25.24	2.05
Slag 4 top	0.21	0.18	0.10	0.74	74.1	23.74	6.36	3.71	3.29	3.26	40.13	43.43	3.53
Slag 4 bottom	0.44	0.71	0.36	6.03	82	8.42	5.86	3.81	6.83	3.33	40.97	47.80	3.89
Slag 5 top	0.36	0.36	0.17	1.28	93	0.70	6.19	3.80	6.74	1.16	14.21	20.95	1.70
Slag 5 bottom	2.91	7.24	3.54	11.26	72.3	7.03	5.81	3.80	39.55	1.09	13.38	52.93	4.30

Table 18: Results of metal droplet analysis.

Figure 63 and 64 depict the true spatial size distributions, as calculated using equation 42, for the bottom and top of Slag 1.

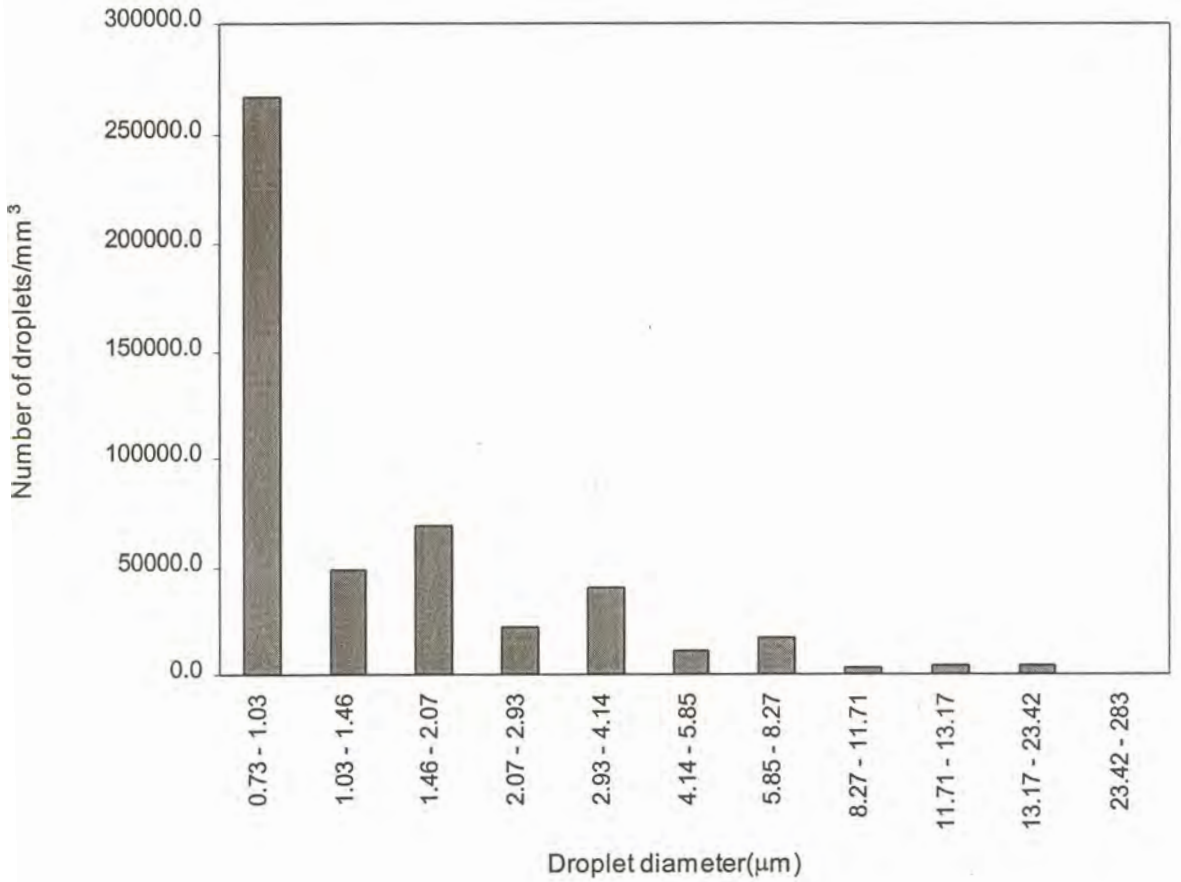

Figure 63: True spatial size distribution of entrained droplets for Slag 1 bottom.

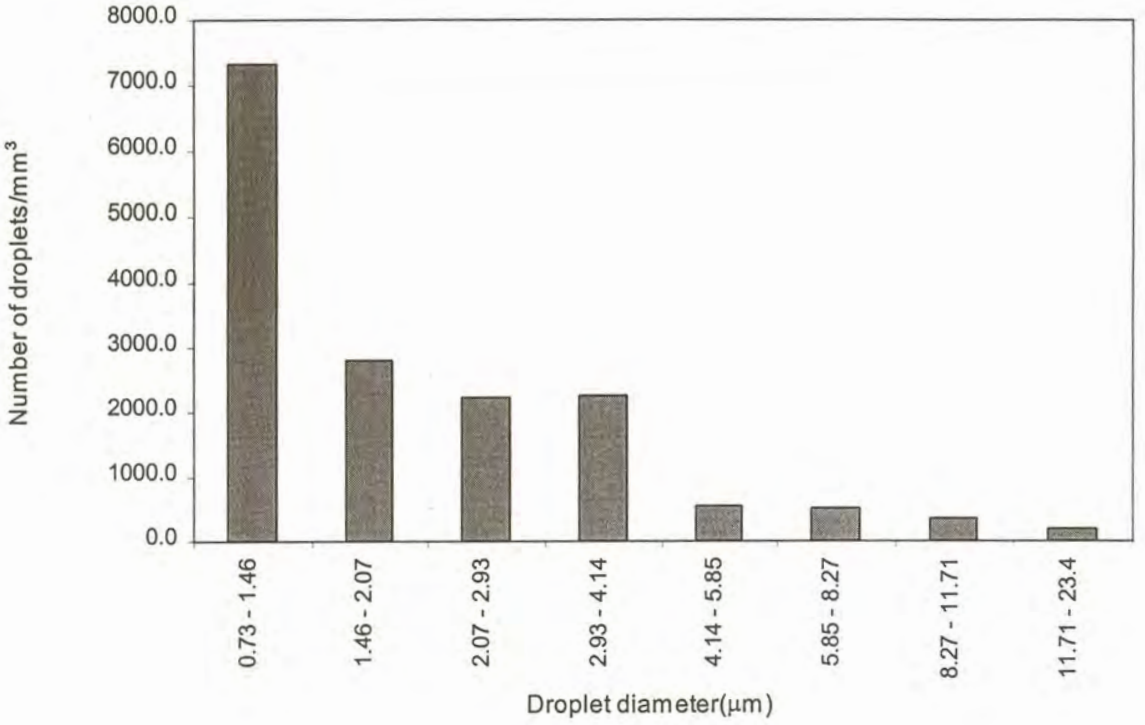

Figure 64: True spatial size distribution of entrained droplets for Slag 1 top.

Figure 65 and 66 depict the volume fraction of particles in each class interval for the bottom and top of slag 1.

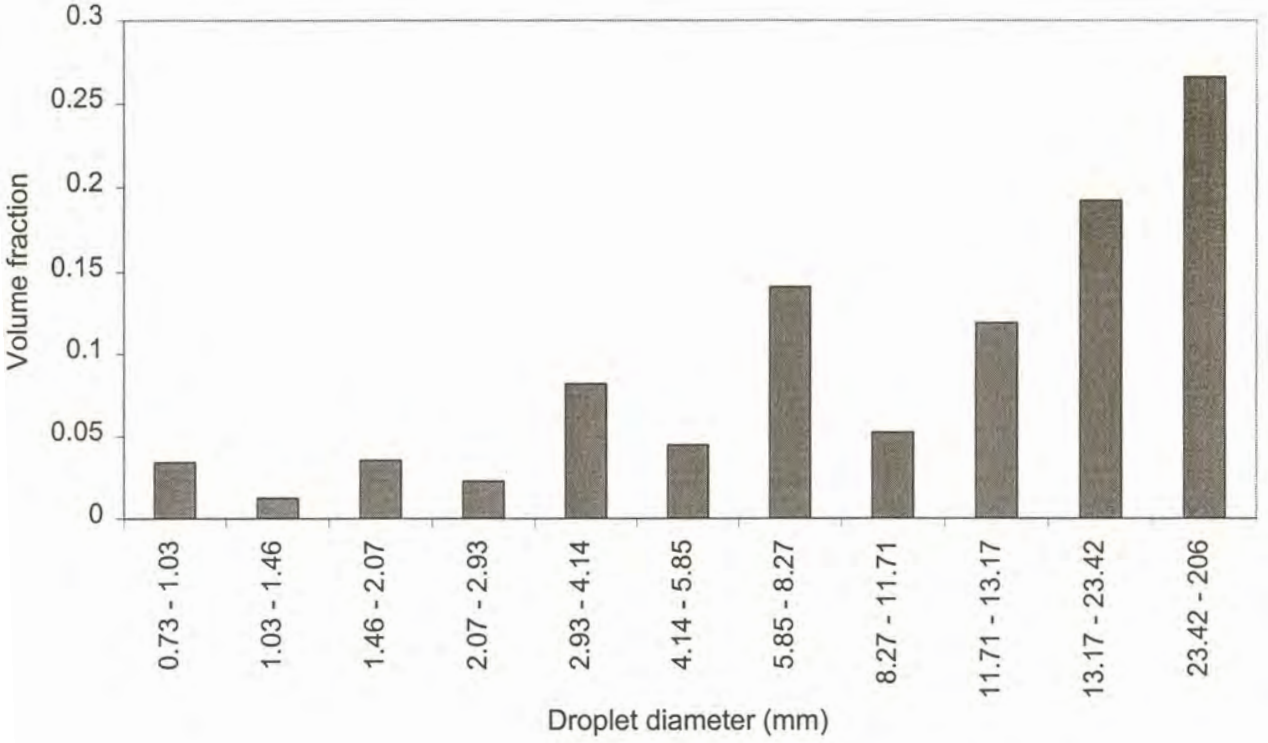

Figure 65: The volume fraction of particles in each class interval for the bottom of Slag 1.

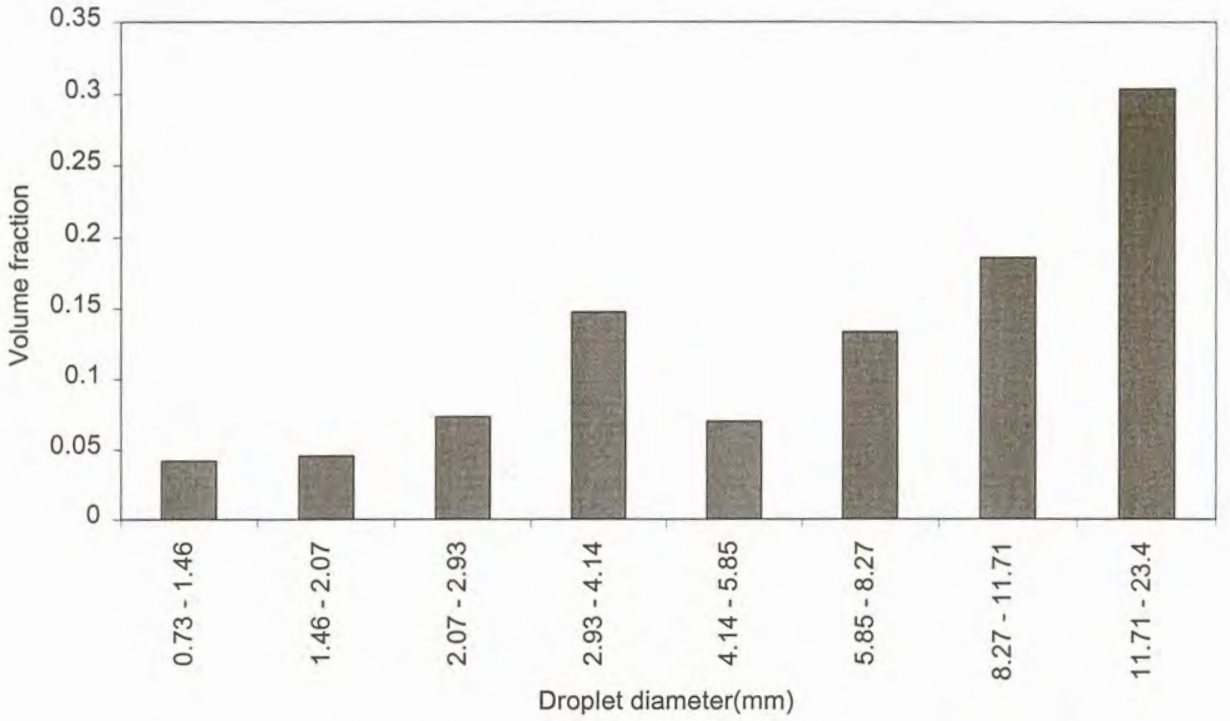

Figure 66: The volume fraction of particles in each class interval for the bottom of Slag 1.

Figures 63 and 64 show that by far the largest number of the metal droplets is smaller than 5 μm and the concentration and size of entrained particles is much larger in case of the bottom slag sample. In contrast to this, figures 65 and 66 show that the largest volume fraction of droplets lies in the class intervals larger than 5 μm. Thus, the mass of entrained metal particles can be estimated by considering only 5 μm particles and larger. Due to the time consuming nature of the droplet size distribution calculations to estimate the volume fraction of the metal particles in the slag, only the area fraction calculations were utilized to estimate the volume fraction of metal particles for the remainder of the slag samples.

The effect of temperature and slag composition on metal droplet entrainment is shown in figure 67.

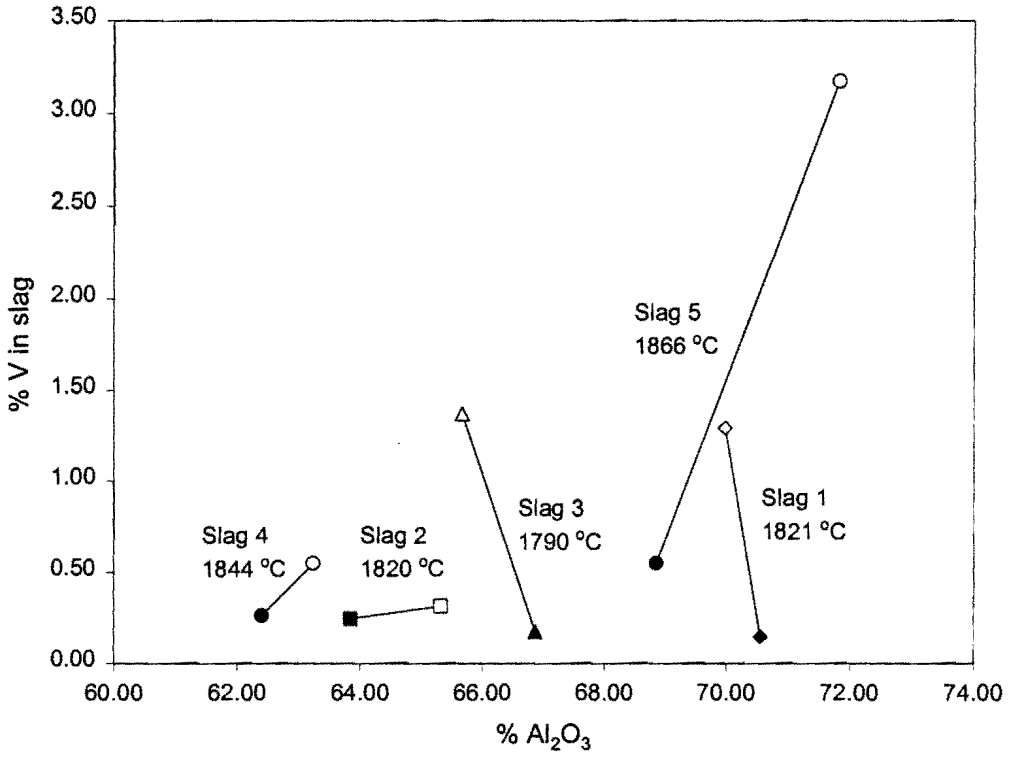

Figure 67: Vanadium losses, with recorded tap temperatures for different slag samples. The % V in the slag is only the vanadium associated with the entrained metal droplets. A slag mass of 1230 kg was assumed. The open data markers and solid data markers present samples taken at the bottom and top of the bulk sample, respectively. The investigations were carried out on the polished sections of which the VO_x content was previously determined. (See section 5.2.2.2)

Before any conclusions relating to the influence of slag composition on droplet entrainment can be drawn, the influence of tap temperature should first be investigated. High tap temperatures will reduce the viscosity and increase the solidification period of the slag, resulting in the reduction of metal droplet entrainment. However, no relation between the amount of droplets entrained and the tap temperature could be observed as

shown in figure 67. The amount of droplets entrained, in this case, is not very sensitive to temperature fluctuations which may be encountered from smelt to smelt (See specially the solid data markers).

Vanadium losses to the slag expressed as % V in metal droplets and total % V in slag (the latter includes oxidic and metallic vanadium) for the top and bottom slag samples, are shown in figure 68 and 69 respectively.

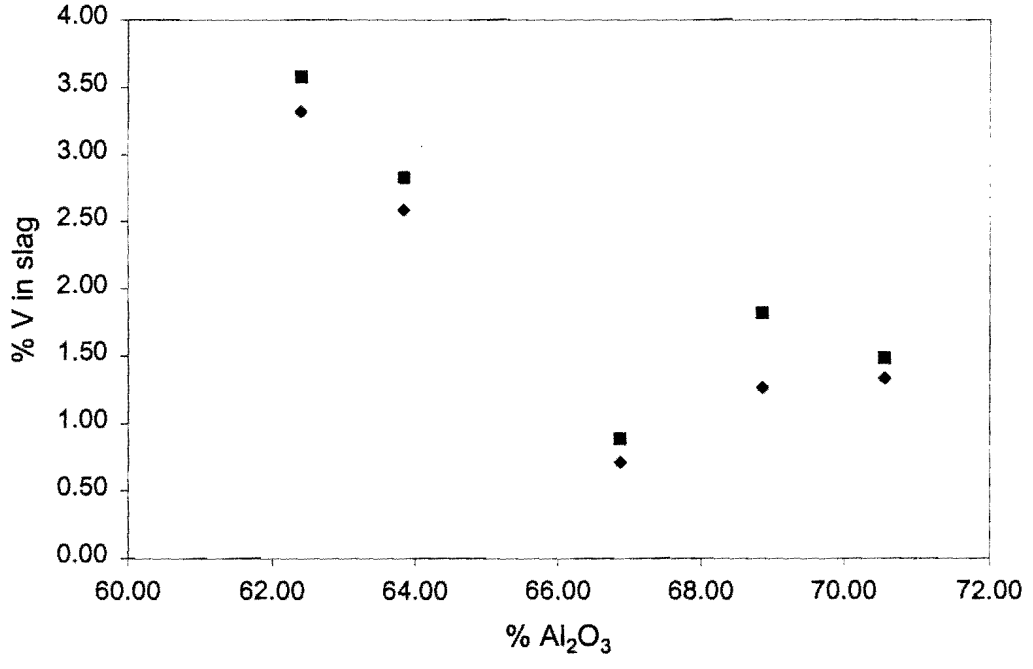

Figure 68: Soluble and total vanadium loss to the slag as function of the slag basicity for the top slag samples. In this figure the squares show the total vanadium composition of the slag (Soluble as well as droplet contributions), and the diamond figures the soluble vanadium content of the slag

Figure 68 indicates that the contribution of the entrained metal particles to the total vanadium loss to the slag is relatively small with the maximum contribution of $\approx$ 0.5 %. This figure depicts, thus, that small adjustments made to the slag basicity by decreasing the fluxing agent additions will increase the metal recoveries. The total vanadium content

of the slag can be reduced from ≈ 3.5 % to ≈ 1.5 % by adjusting the alumina composition from ≈ 60 % to 70 %. Figure 68 appears to have a minimum at around 67 % alumina resulting in a total vanadium loss around 1 %, but this can only confirmed if more analyses on industrial samples are conducted. Nevertheless, higher slag viscosity which is a result of a higher liquidus temperatures appears not to be strongly affecting the entrainment of metal particles for slag samples taken from the top of the industrial bulk slag samples.

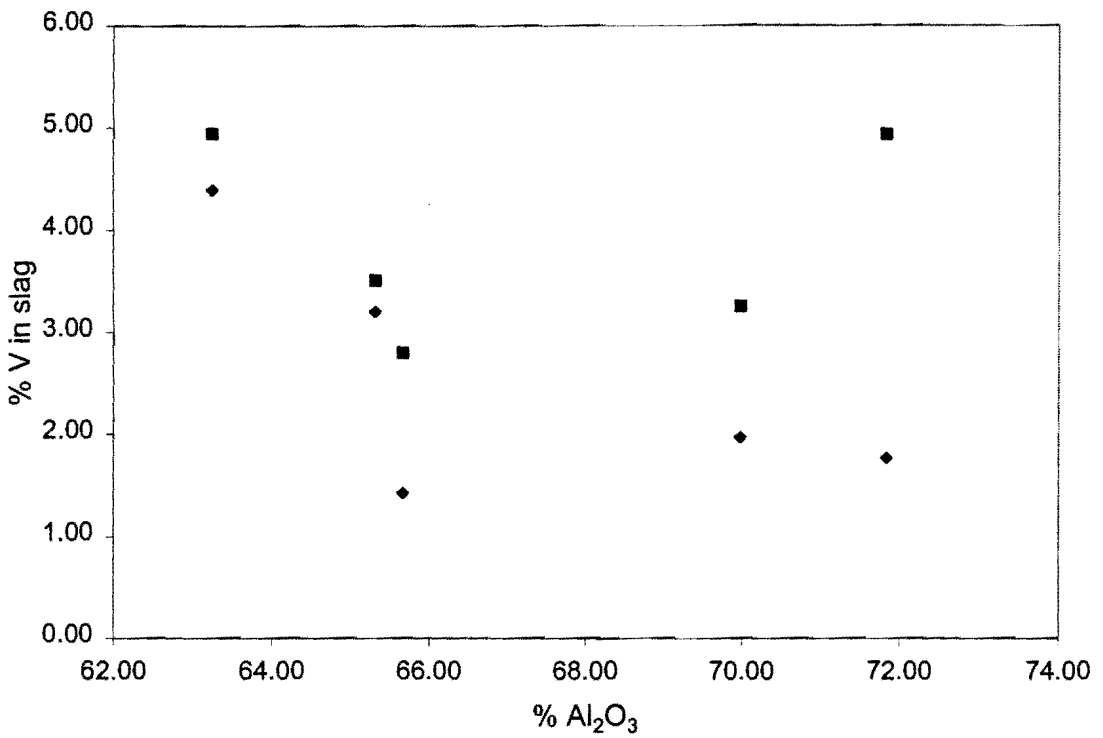

Figure 69: Soluble and total vanadium loss to the slag as function of the slag basicity of the bottom slag samples. In this figure the squares show the total vanadium composition of the slag (Soluble as well as droplet contributions), and the diamond symbols the soluble vanadium content of the slag

Compared to figure 68, figure 69 shows a very strong effect of the slag basicity on the amount of vanadium associated with the entrained metal particles with the maximum around 3.3 %. At this stage, it is worth mentioning that slag samples were taken very

close to the slag-metal interface. The amount of entrained droplets was very dependent on the height within the bulk sample. The first few centimeters along the y-axis of the sample contained most of the entrained droplets, whereafter the concentration strongly declined further along the y-axis. The very high concentration of the droplets close to the interface give rise to unusually high losses of vanadium to the entrained metal particles which are not representative of the entire bulk slag sample. The crowding of the droplets close to the interface should be avoided as far as representative sampling is concerned because this effect is only observed for a very small fraction of the total slag volume.

The influence of slag basicity on metal droplet entrainment is thus better depicted by figure 68 than figure 69. In addition to this, the amount of entrained droplets is also strongly dependent on the horizontal position within the bulk slag sample. Slag closer to the slag pot lining solidifies more rapidly than slag closer to the center, resulting in a higher concentration of metal particles closer to the lining.

It can be concluded from the results that vanadium losses as entrained droplets could not be fully quantified by analyzing samples from the top and bottom of the bulk slag sample. Although the samples taken at the top of the bulk slag sample are expected to be more representative of the entire slag sample, the positional effect on droplet entrainment introduces much uncertainty. In order to fully quantify metal droplet entrainment as a possible cause of vanadium loss to the slag, new sampling methods must be derived. One such way is to sample from both the y and x direction to establish a three-dimensional mapping of the bulk slag sample. Only then will the positional effect on droplet entrainment be fully quantified. A number of slag samples should be subjected to this extended sampling to establish the effect of slag composition on metal droplet entrainment.